

## Electronic Supplementary Information

### **g-C<sub>3</sub>N<sub>4</sub> nanosheets-based ratiometric fluorescent probe for the amplification and imaging of miRNA in living cells**

*Yi-Ting Wang<sup>†</sup>, Na Wu, Feng-Na Guo, Rui-Xue Gao, Ting Yang\*, Jian-Hua Wang\**

Research Center for Analytical Sciences, Department of Chemistry, College of Sciences, Box 332, Northeastern University, Shenyang 110819, China

E-mail address: [yangting@mail.neu.edu.cn](mailto:yangting@mail.neu.edu.cn), [jianhuajrz@mail.neu.edu.cn](mailto:jianhuajrz@mail.neu.edu.cn).

## Electronic Supplementary Information Included:

### 1. Experimental details

1.1 Chemicals and materials.

1.2 Instrumentations.

### 2. Supplemental tables and figures

**Table S1.** Sequences of nucleic acid.

**Table S2.** The analysis results of miR-582-3p content in cell lysates (n=3).

**Figure S1.** PAGE (12%) gel electrophoresis analysis of HCR reaction. Lane 1, target miRNA (1.2  $\mu\text{mol L}^{-1}$ ); lane 2, H1-CuNCs (1.2  $\mu\text{mol L}^{-1}$ ); lane 3, H2-CuNCs (1.2  $\mu\text{mol L}^{-1}$ ); lane 4, 1.2  $\mu\text{mol L}^{-1}$  H1-CuNCs mixed with 1.2  $\mu\text{mol L}^{-1}$  H2-CuNCs; lane 5-9, the HCR products. The concentrations of H1-CuNCs and H2-CuNCs used from lane 5 to 9 are 0.4, 0.8, 1.2, 1.8 and 2.4  $\mu\text{mol L}^{-1}$ , respectively, with 1.2  $\mu\text{mol L}^{-1}$  target miRNA. The gel was run at 180 V for 30 min in TBE buffer.

**Figure S2.** The emission spectra of BCNNS (100  $\mu\text{g mL}^{-1}$ ) at various excitation wavelengths.

**Figure S3.** The variation of fluorescence intensity of CuNCs (100  $\text{nmol L}^{-1}$ ) as a function of ionic strength with excitation at  $\lambda_{\text{ex}}$  340 nm.

**Figure S4.** The variation of fluorescence intensity of BCNNS ( $100 \mu\text{g mL}^{-1}$ ) as a function of ionic strength with excitation at  $\lambda_{\text{ex}}$  340 nm.

**Figure S5.** The variation of fluorescence intensity of BCNNS ( $100 \mu\text{g mL}^{-1}$ ) as a function of pH value with excitation at  $\lambda_{\text{ex}}$  340 nm.

**Figure S6.** The variation of fluorescence intensity of BCNNS ( $100 \mu\text{g mL}^{-1}$ ) as a function of irradiation time with excitation at  $\lambda_{\text{ex}}$  340 nm.

**Figure S7.** Quenching effect of BCNNS at various concentrations on CuNCs. The concentration of CuNCs is  $100 \text{ nmol L}^{-1}$ . BCNNS concentrations are given within a range of  $0\text{-}200 \mu\text{g mL}^{-1}$ . The excitation and emission wavelengths are set at 340 and 600 nm, respectively.

**Figure S8.** Quenching effect of BCNNS on the fluorescence of CuNCs with various concentrations. The concentration of BCNNS is  $200 \mu\text{g mL}^{-1}$ . CuNCs concentrations are given in a range of  $0\text{-}200 \text{ nmol L}^{-1}$ . The excitation and emission wavelengths are set at 340 and 600 nm, respectively.

**Figure S9.** Time-dependent fluorescence changes of BCNNS-CuNCs in the presence of miR-582-3p ( $10 \text{ pmol L}^{-1}$ ). The excitation and emission wavelengths are set at 340 and 600 nm, respectively.

**Figure S10.** The fluorescence response of the system in the presence of miR-582-3p ( $10 \text{ pmol L}^{-1}$ ) under different conditions: BCNNS-H1/H2-CuNCs; BCNNS-H1-CuNCs; BCNNS-H2-CuNCs; BCNNS-H1/H2-CuNCs-miR-582-3p; BCNNS-H1-CuNCs-miR-582-3p; H1/H2-CuNCs-miR-582-3p and BCNNS-miR-582-3p. The concentrations of H1/H2-CuNCs, H1-CuNCs and H2-CuNCs are  $100 \text{ nmol L}^{-1}$ ; the concentration of BCNNS is  $200 \mu\text{g mL}^{-1}$ .

**Figure S11.** Effect of the BCNNS-CuNCs concentration ( $0, 2, 5, 10, 20, 50, 100, 200$  and  $500 \mu\text{g mL}^{-1}$ ) on the viability of A549 cells with an incubation

time of 24 h.

**Figure S12.** Effect of the BCNNS-CuNCs concentration (0, 2, 5, 10, 20, 50, 100, 200 and 500  $\mu\text{g mL}^{-1}$ ) on the viability of BEAS-2B cells with an incubation time of 24 h.

**Figure S13.** Confocal images of A549 cells incubated with BCNNS-CuNCs (200  $\mu\text{g mL}^{-1}$ ) for 0, 1, 2, 3, 4 and 5 h. Scale bar: 40  $\mu\text{m}$ .

**Figure S14.** The calibration curve between miR-582-3p mimics concentration and relative optical density (red channel *vs* blue channel).

## 1. Experimental details

### 1.1 Chemicals and materials.

All the nucleic acids used in this study were custom-designed and synthesized by Sangon Biological Engineering Technology & Services Co. Ltd (Shanghai, China).

The sequences of nucleic acids were listed in Table S1. Thiourea,  $H_3BO_3$ ,  $CuSO_4 \cdot 5H_2O$ , NaCl, KCl,  $MgCl_2$ , NaOH, HCl,  $H_3PO_4$ ,  $CH_3COOH$ ,  $NaHPO_4 \cdot 12H_2O$ ,  $KH_2PO_4$ ,  $HNO_3$ , dimethyl sulfoxide (DMSO) were provided by Sinopharm Chemical Reagent Co. Ltd (Shanghai, China). 3-Morpholinopropanesulfoinic acid (MOPS) and tris-base were the products of Aladdin Bio-Chem Technology Co., Ltd (Shanghai, China). Dulbecco's modified Eagle's medium (DMEM, high glucose), fetal bovine serum, penicillin, streptomycin and trypsin (0.25%) were obtained from Hyclone (Thermo Scientific, USA). 3-(4,5-dimethylthiazol-2-yl)-2,5-diphenyl tetrazolium bromide (MTT) assay kit was acquired from KeyGEN Biotech Co. Ltd (Nanjing, China). Entranster<sup>TM</sup>-R4000 transfection reagent was purchased from Engreen Biosystem Co, Ltd (Beijing, China). All the chemicals were used as received and deionized water ( $18\text{ M}\Omega\text{ cm}^{-1}$ ) was used throughout.

### 1.2 Instrumentations.

The morphology of copper nanocluster (CuNCs) and boron doped g- $C_3N_4$  nanosheets (BCNNS) were studied by a JEM-ARM 200F high-resolution transmission electron microscope (JEOL Ltd.) and a Tecnai G220 field-emission electron microscope (FEI, America). Atomic force microscopy (AFM) image was acquired on a Bruker Dimension icon atomic force microscopy (Bruker, Germany)

using tapping mode. X-ray diffraction (XRD) was characterized with an MPDDY2094 X-ray diffractometer (PANalytical B.V., Netherlands) with Cu-K $\alpha$  irradiation ( $\lambda=1.5406 \text{ \AA}$ ) in a range of  $2\theta=5-80^\circ$ . X-ray photoelectron spectra (XPS) analyses were carried out on an ESCALAB 250 X-ray photoelectron spectroscopy (Thermo Instruments Inc., USA) with monochromated Al K $\alpha$  280.00 eV excitation source. UV-vis absorption spectra were measured on a U-3900 spectrophotometer (Hitachi High Technologies, Japan). Fluorescence (FL) measurements were carried on an F-7000 fluorescence spectrometer (Hitachi High Technologies, Japan) with a 0.5 cm optical path, a scan speed of  $1200 \text{ nm min}^{-1}$  and 10.0 nm slits for both excitation and emission. Inductively coupled plasma mass spectrometer (ICP-MS, Agilent 8900, Agilent Technologies, CA, USA) was used for the quantification of target miRNA by detecting the isotope of  $^{63}\text{Cu}$ . MTT assay was performed on a Synergy H1 ELISA plate reader (BioTek Instruments Inc., USA). Fluorescence images of cells were taken by an FV 1200 confocal laser scanning microscopy (Olympus, Japan) with a 40 $\times$ objective lens.



Table S2. The analysis results of miR-582-3p content in cell lysates (n=3).

Sample	Found (nmol L <sup>-1</sup> )	Spiked (nmol L <sup>-1</sup> )	Recovery (%)
Lysate 1*	12.0±2.5	5	93±13
		10	102±12
		20	91±6
Lysate 2*	20.5±2.0	5	103±17
		10	90±5
		20	106±5

\* The amount of the cells in lysate 1 and 2 were  $2.10 \times 10^6$  and  $2.65 \times 10^6$ , respectively.

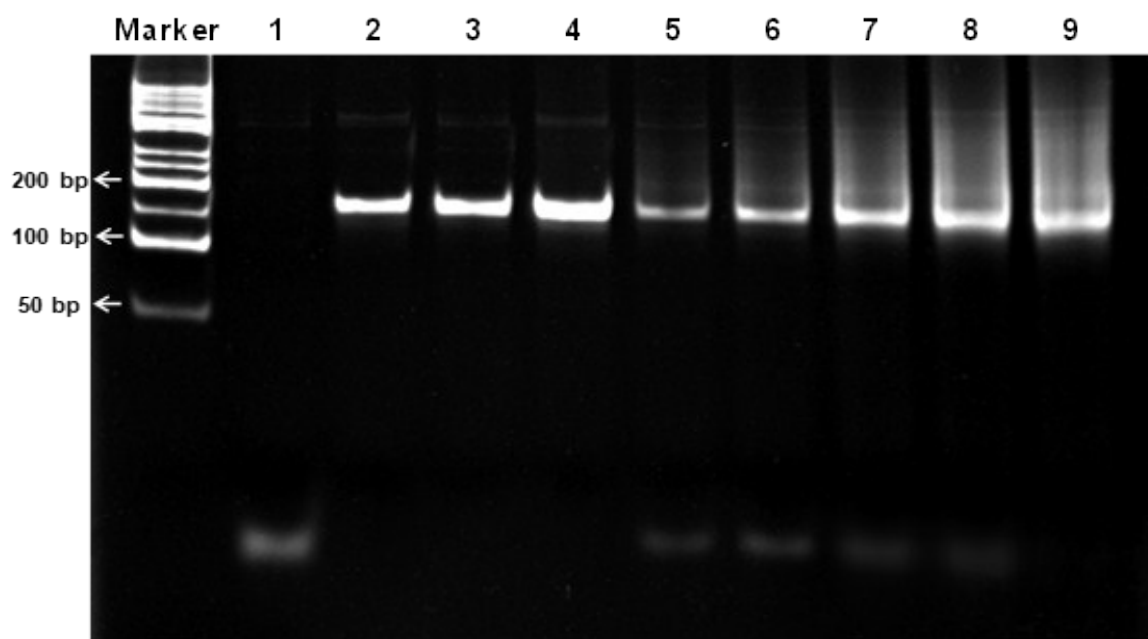


Figure S1. PAGE (12%) gel electrophoresis analysis of HCR reaction. Lane 1, target miRNA ( $1.2 \mu\text{mol L}^{-1}$ ); lane 2, H1-CuNCs ( $1.2 \mu\text{mol L}^{-1}$ ); lane 3, H2-CuNCs ( $1.2 \mu\text{mol L}^{-1}$ ); lane 4,  $1.2 \mu\text{mol L}^{-1}$  H1-CuNCs mixed with  $1.2 \mu\text{mol L}^{-1}$  H2-CuNCs; lane 5-9, the HCR products. The concentrations of H1-CuNCs and H2-CuNCs used from lane 5 to 9 are  $0.4$ ,  $0.6$ ,  $1.2$ ,  $1.8$  and  $2.4 \mu\text{mol L}^{-1}$ , respectively, with  $1.2 \mu\text{mol L}^{-1}$  target miRNA. The gel was run at  $180 \text{ V}$  for  $30 \text{ min}$  in TBE buffer.



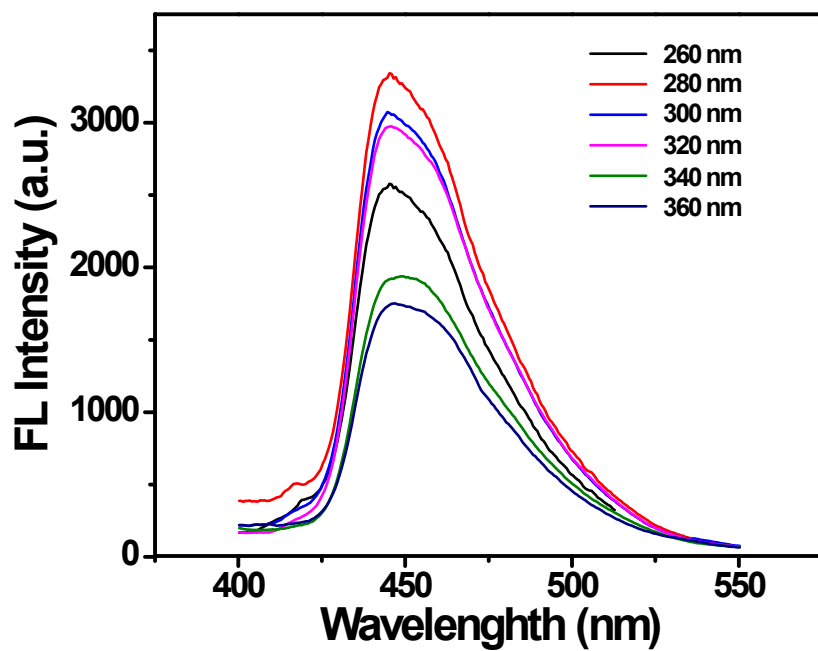


Figure S2. The emission spectra of BCNNS ( $100 \mu\text{g mL}^{-1}$ ) at various excitation wavelengths.

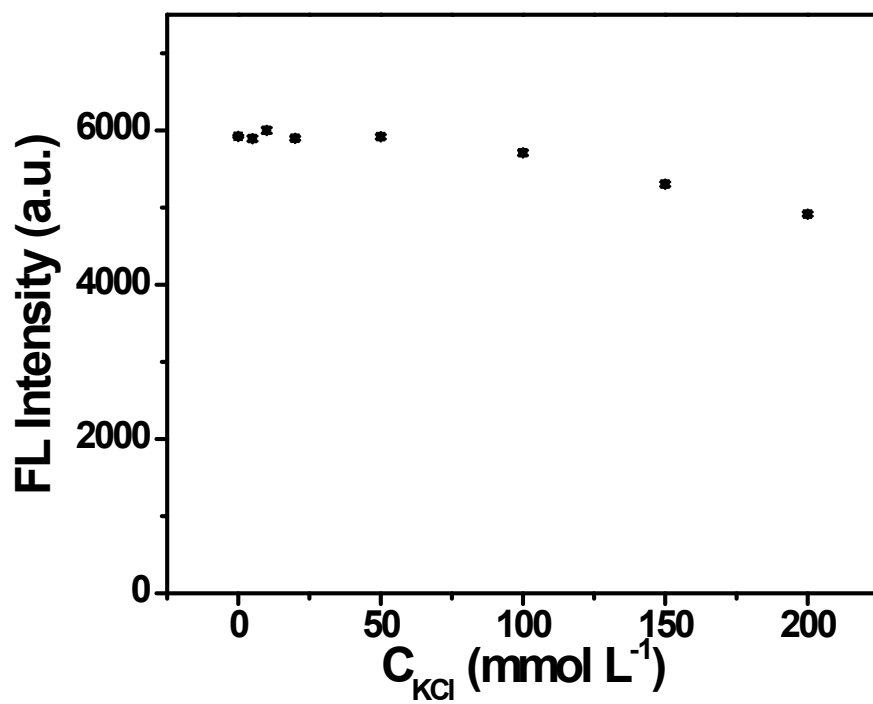


Figure S3. The variation of fluorescence intensity of CuNCs (100 nmol L<sup>-1</sup>) as a function of ionic strength with excitation at  $\lambda_{\text{ex}}$  340 nm.

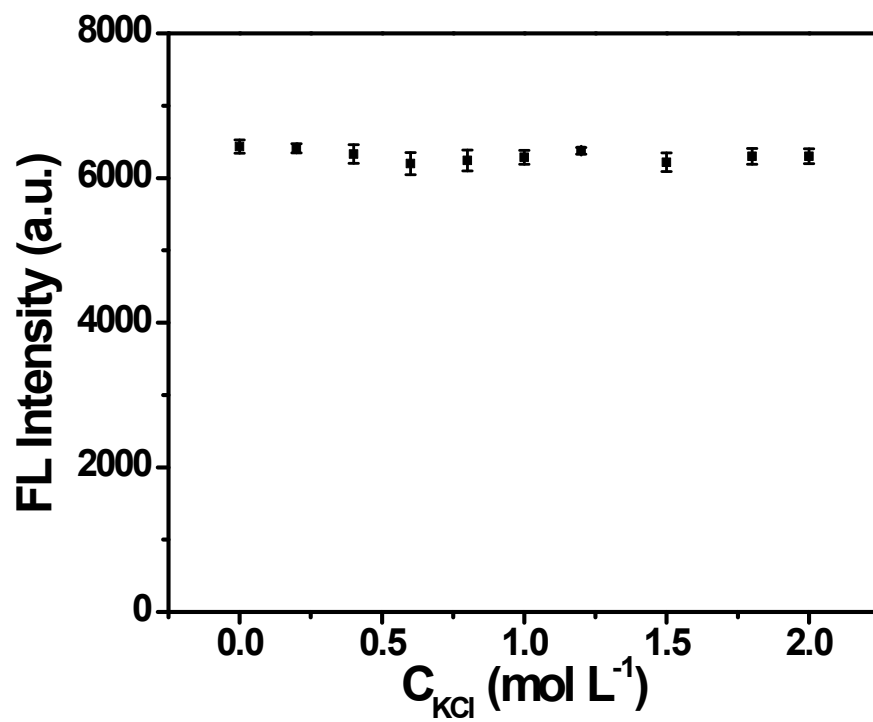


Figure S4. The variation of fluorescence intensity of BCNNS (100  $\mu\text{g mL}^{-1}$ ) as a function of ionic strength with excitation at  $\lambda_{\text{ex}}$  340 nm.

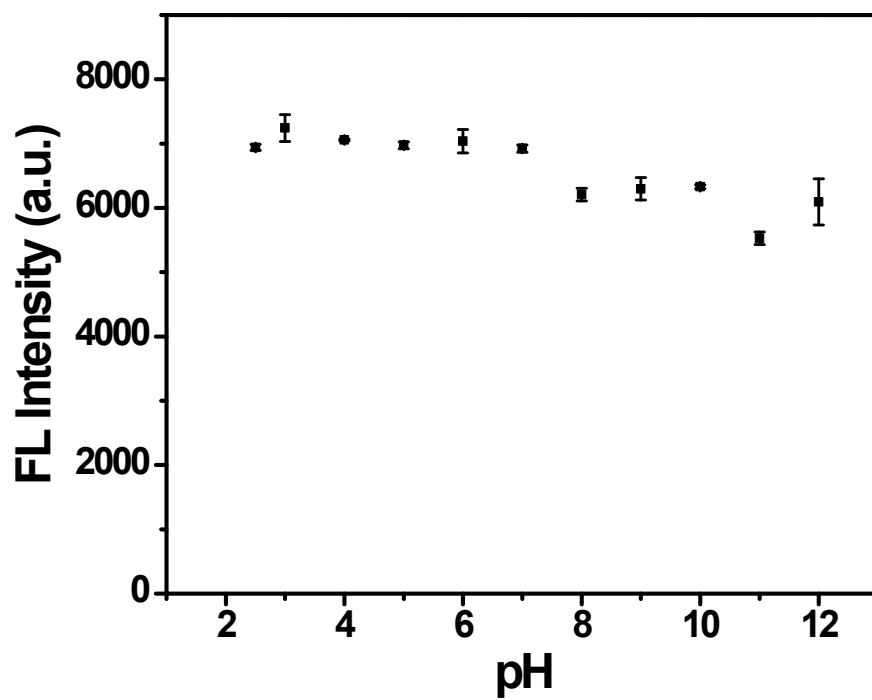


Figure S5. The variation of fluorescence intensity of BCNNS ( $100 \mu\text{g mL}^{-1}$ ) as a function of pH value with excitation at  $\lambda_{\text{ex}}$  340 nm.

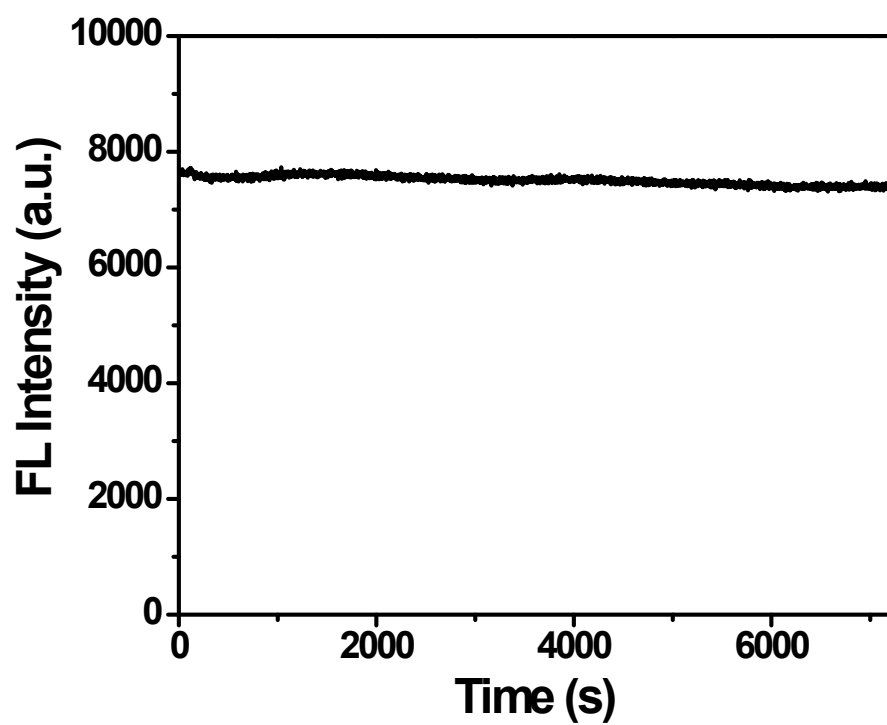


Figure S6. The variation of fluorescence intensity of BCNNS ( $100 \mu\text{g mL}^{-1}$ ) as a function of irradiation time with excitation at  $\lambda_{\text{ex}}$  340 nm.

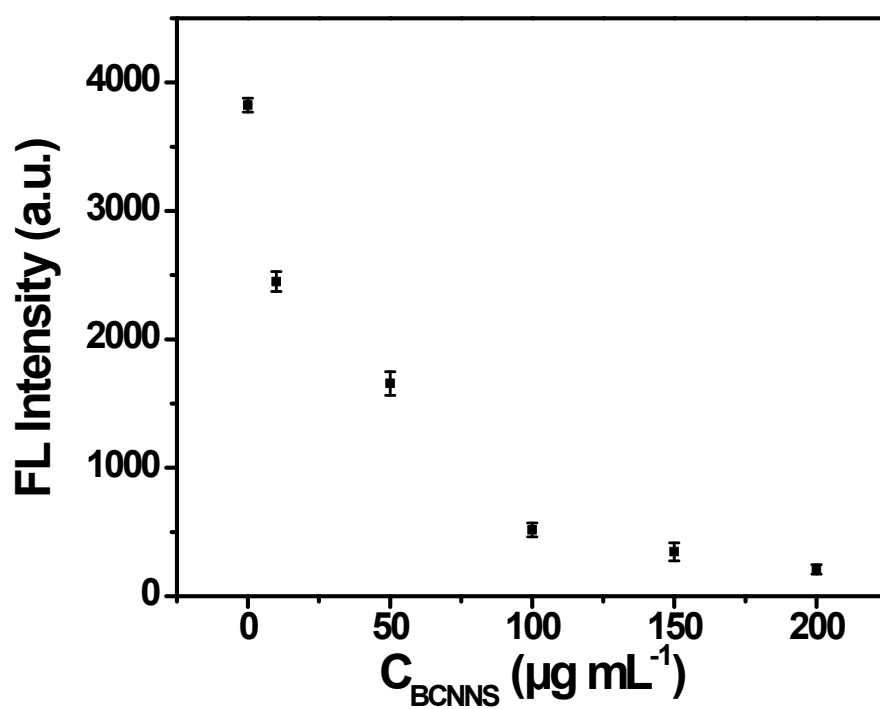


Figure S7. Quenching effect of BCNNS at various concentrations on CuNCs. The concentration of CuNCs is  $100 \text{ nmol L}^{-1}$ . BCNNS concentrations are given within a range of  $0\text{-}200 \mu\text{g mL}^{-1}$ . The excitation and emission wavelengths are set at 340 and 600 nm, respectively.

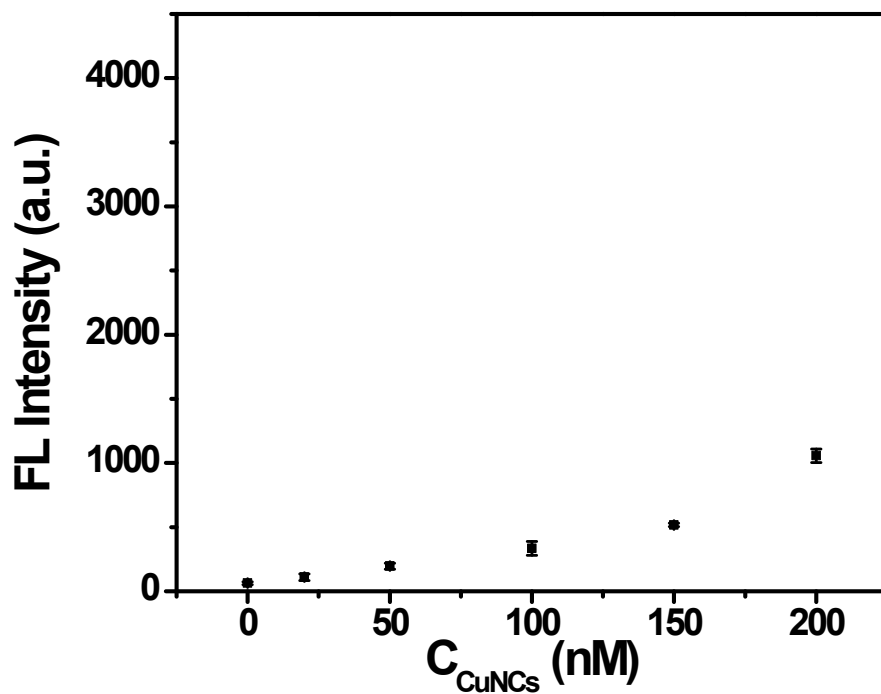


Figure S8. Quenching effect of BCNNS on the fluorescence of CuNCs with various concentrations. The concentration of BCNNS is  $200 \mu\text{g mL}^{-1}$ . CuNCs concentrations are given in a range of  $0\text{-}200 \text{ nmol L}^{-1}$ . The excitation and emission wavelengths are set at  $340$  and  $600 \text{ nm}$ , respectively.

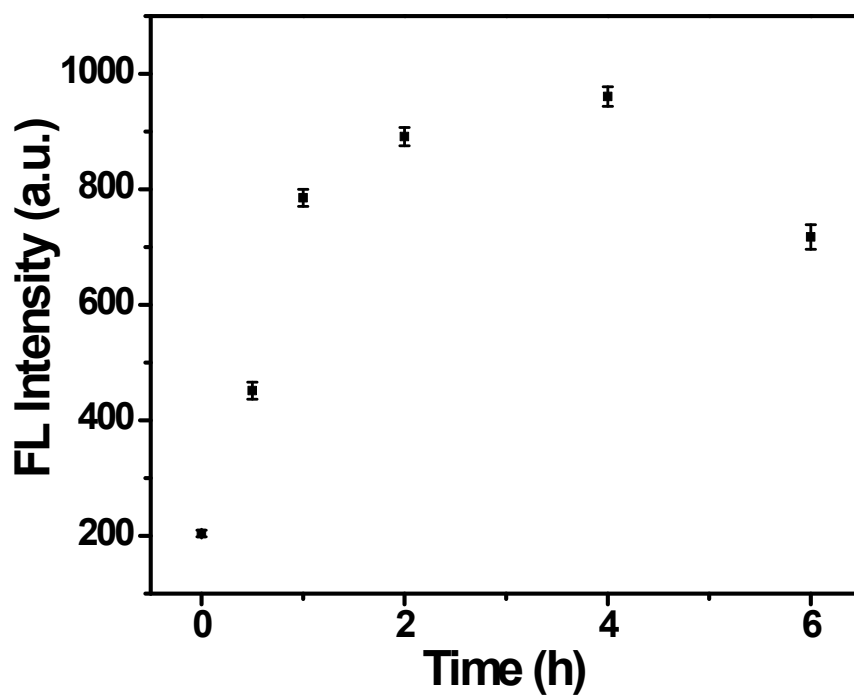


Figure S9. Time-dependent fluorescence changes of BCNNS-CuNCs in the presence of miR-582-3p ( $10 \text{ pmol L}^{-1}$ ). The excitation and emission wavelengths are set at 340 and 600 nm, respectively.



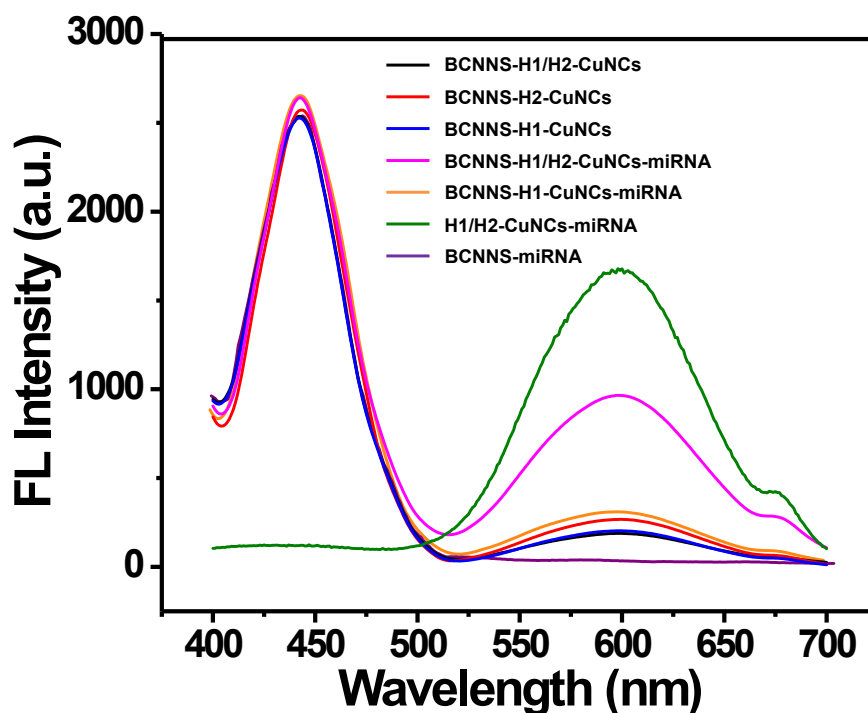


Figure S10. The fluorescence response of the system in the presence of miR-582-3p ( $10 \text{ pmol L}^{-1}$ ) under different conditions: BCNNS-H1/H2-CuNCs; BCNNS-H1-CuNCs; BCNNS-H2-CuNCs; BCNNS-H1/H2-CuNCs-miR-582-3p; BCNNS-H1-CuNCs-miR-582-3p; H1/H2-CuNCs-miR-582-3p and BCNNS-miR-582-3p. The concentrations of H1-CuNCs and H2-CuNCs are  $100 \text{ nmol L}^{-1}$ ; the concentration of BCNNS is  $200 \text{ }\mu\text{g mL}^{-1}$ .

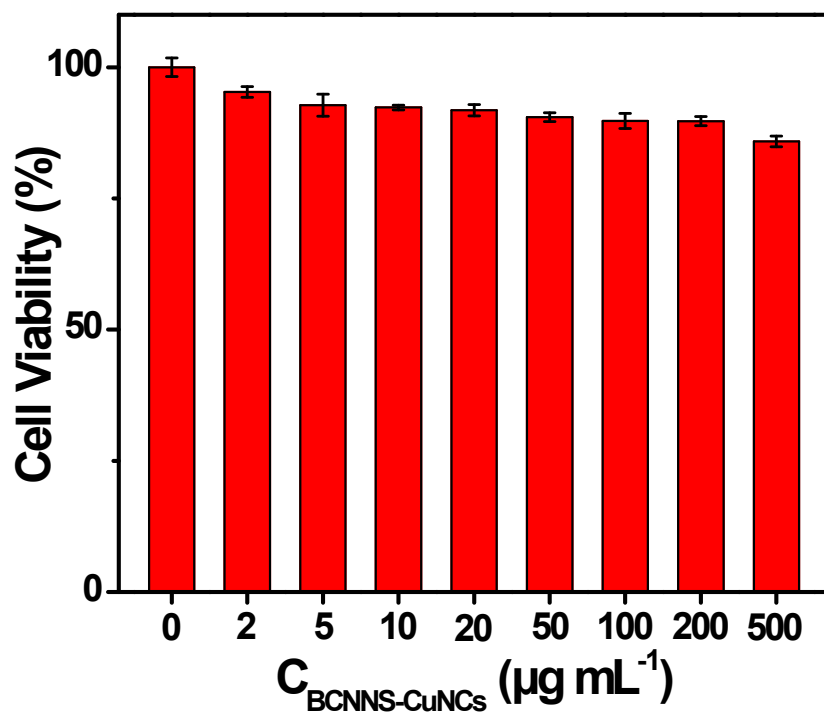


Figure S11. Effect of the BCNNS-CuNCs concentration (0, 2, 5, 10, 20, 50, 100, 200 and 500 µg mL<sup>-1</sup>) on the viability of A549 cells with an incubation time of 24 h.

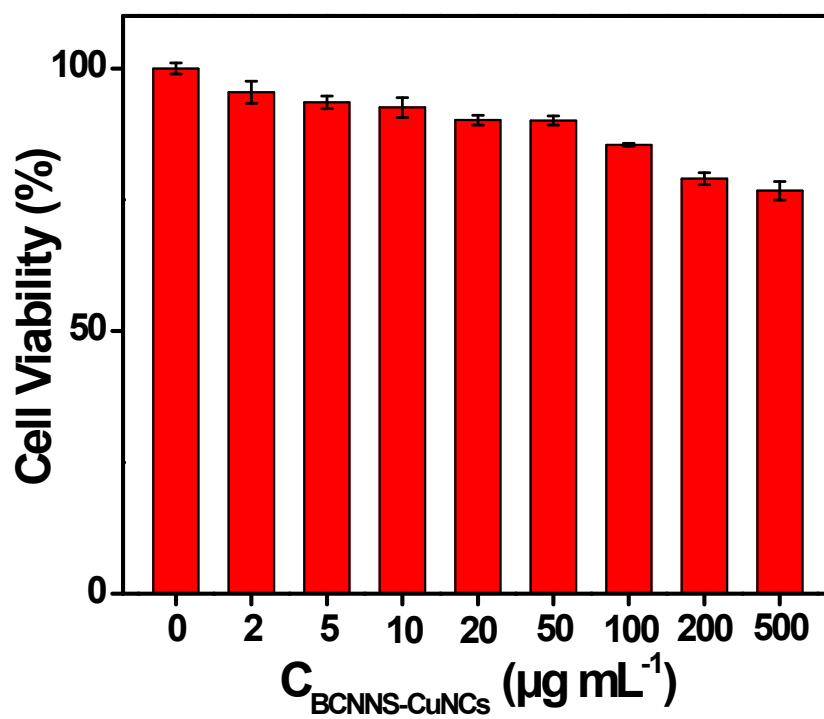


Figure S12. Effect of the BCNNS-CuNCs concentration (0, 2, 5, 10, 20, 50, 100, 200 and 500 µg mL<sup>-1</sup>) on the viability of BEAS-2B cells with an incubation time of 24 h.

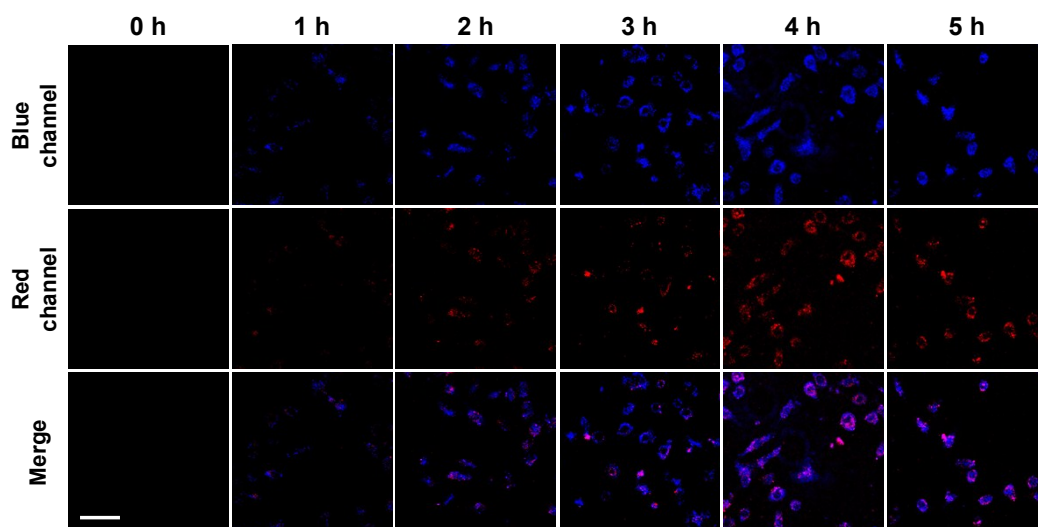


Figure S13. Confocal images of A549 cells incubated with BCNNS-CuNCs ( $200 \mu\text{g mL}^{-1}$ ) for 0, 1, 2, 3, 4 and 5 h. Scale bar:  $40 \mu\text{m}$ .

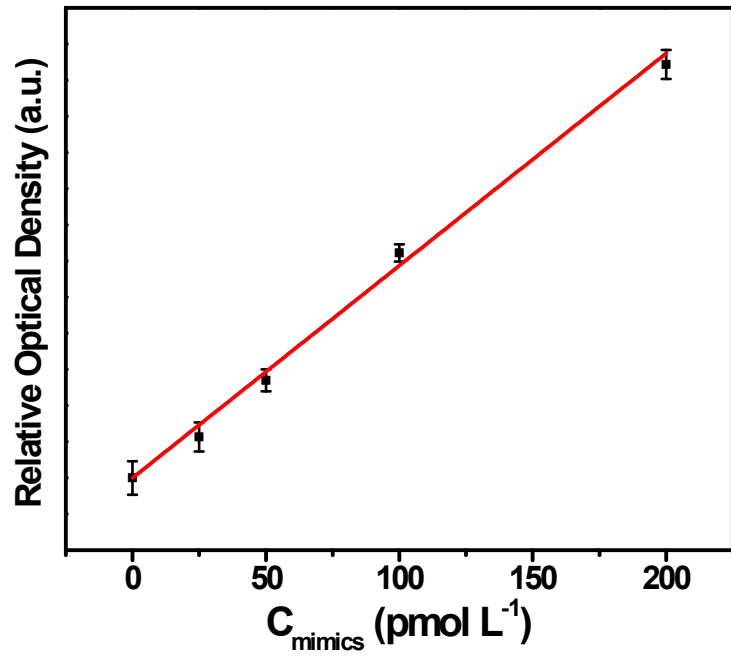


Figure S14. The calibration curve between miR-582-3p mimics concentration and relative optical density (red channel vs blue channel).